Volume 17 | Number 34 | 14 September 2015 | Pages 6459–6608

CrystEngComm

www.rsc.org/crystengcomm

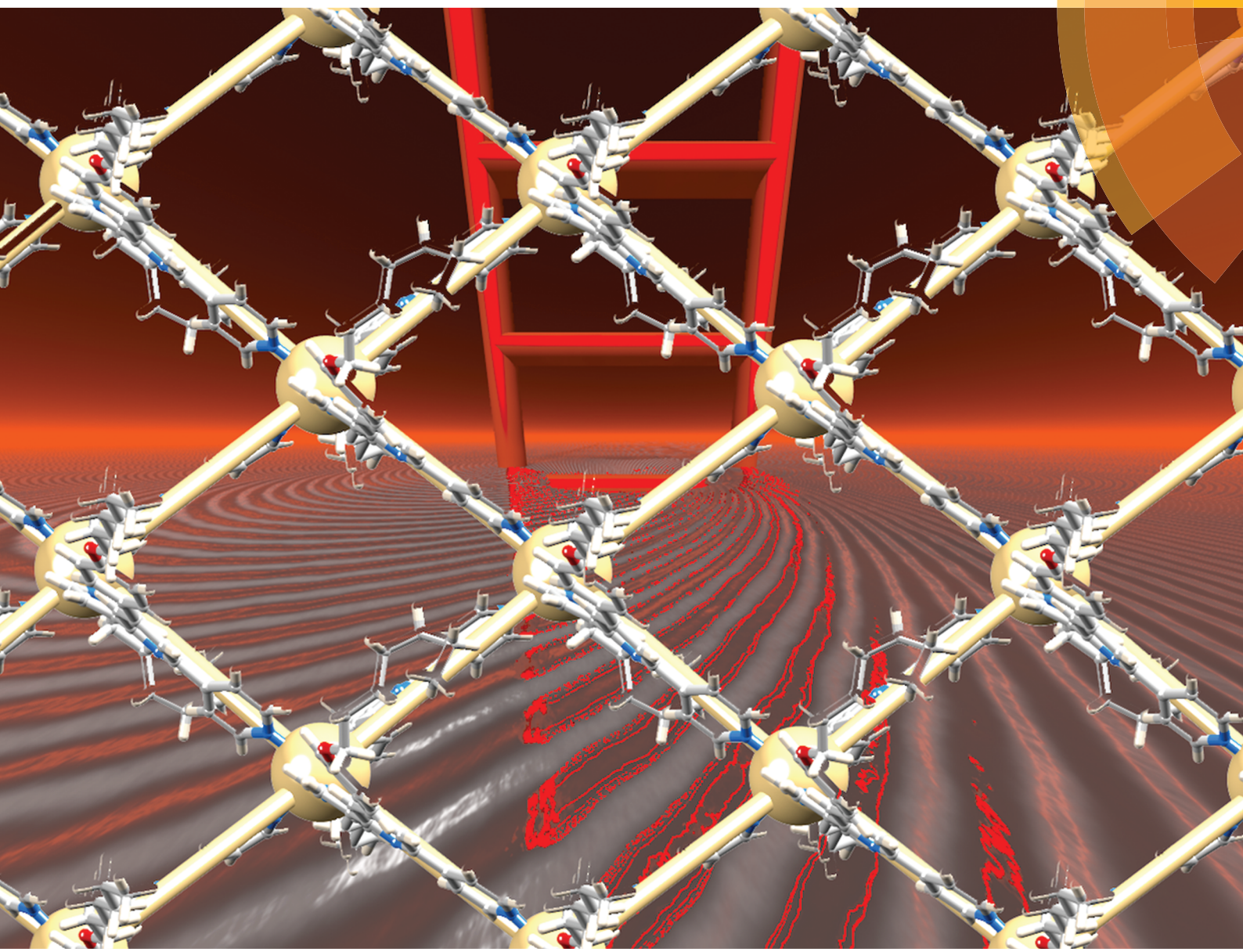

ROYAL SOCIETY OF CHEMISTRY

PAPER

Catherine E. Housecroft *et al.*

Manipulating connecting nodes through remote alkoxy chain variation in coordination networks with 4′-alkoxy-4,2′:6′,4″-terpyridine linkers

CrystEngComm

PAPER

View Article Online
View Journal | View Issue

Cite this: *CrystEngComm*, 2015, **17**, 6483

Manipulating connecting nodes through remote alkoxy chain variation in coordination networks with 4′-alkoxy-4,2′:6′,4″-terpyridine linkers†

Y. Maximilian Klein, Alessandro Prescimone, Edwin C. Constable and Catherine E. Housecroft*

The effects of increasing the length of the alkoxy substituent in 4′-alkoxy-4,2′:6′,4″-terpyridines when they are combined with cadmium(II) nitrate under conditions of room temperature crystallization and in the same cadmium : ligand (1 : 3) ratio have been investigated. The divergent ligand 4′-*n*-propoxy-4,2′:6′,4″-terpyridine (**2**) reacts with $Cd(NO_3)_2{\cdot}4H_2O$ to give $[\{Cd_2(NO_3)_4(\mathbf{2})_3\}{\cdot}3CHCl_3]_n$ in which the Cd atoms act as 3-connecting nodes and assemble into a (6,3) net with each ligand **2** linking adjacent Cd atoms. One of the three independent *n*-propoxy groups nestles into a cleft in the next 2-dimensional sheet; this 'tail-in-pocket' interaction restricts the length of the alkyl chain that can be accommodated. Replacing the *n*-propoxy by an *n*-pentoxy, *n*-hexoxy or *n*-heptoxy substituent results in a switch from a (6,3) to (4,4) net; in $[\{Cd_2(NO_3)_4(\mathbf{3})_4\}{\cdot}3CHCl_3]_n$ (**3** = 4′-*n*-pentoxy-4,2′:6′,4″-terpyridine) and $[\{Cd_2(NO_3)_4(\mathbf{4})_4\}{\cdot}CHCl_3{\cdot}MeOH]_n$ (**4** = 4′-*n*-hexoxy-4,2′:6′,4″-terpyridine), each Cd atom is a 4-connecting node with *trans*-nitrato ligands, while in $[\{Cd(NO_3)_2(\mathbf{5})_2\}{\cdot}2MeOH]_n$ (**5** = 4′-*n*-heptoxy-4,2′:6′,4″-terpyridine) a *cis*-arrangement of nitrato ligands is observed. The reaction between $Cd(NO_3)_2{\cdot}4H_2O$ and **4** was also investigated using a 1 : 1 ratio of reagents; this leads to the assembly of the 1-dimensional ladder $[Cd_2(NO_3)_4(MeOH)(\mathbf{4})_3]_n$ in which each Cd atom is a 3-connecting node. In each structure, face-to-face π-stacking of the central pyridine rings or of pyridine/phenyl rings of ligands in adjacent sheets or chains is a primary packing interaction; the role of van der Waals interactions as the chain length increases is discussed. Powder diffraction confirmed that each coordination polymer or network characterized by single crystal X-ray crystallography was representative of the bulk sample. The solid-state emission properties of ligands **2**, **3** and **4** and their coordination polymers are reported; the blue emission of the free ligands is red-shifted by up to 59 nm upon formation of the coordination networks, and quantum yields are in the range 11–22%.

Received 8th June 2015,
Accepted 26th June 2015

DOI: 10.1039/c5ce01115a

www.rsc.org/crystengcomm

Introduction

Diversity in the architectures of 2- and 3-dimensional coordination polymers is engineered through the use of complementary metal nodes and organic (ligand) linkers.[1–7] Oligopyridines remain popular tectons in supramolecular assemblies,[8,9] and over the last 15 years, the divergent 4,2′:6′,4″-terpyridine (4,2′:6′,4″-tpy) domain has proved to be a versatile linker[10] binding metal ions through the outer pyridine rings (Scheme 1). 4,2′:6′,4″-Terpyridines are easily functionalized in the 4′-position to incorporate additional coordination sites[11] or sterically variable substituents (*e.g.* bulky[12] or long chain,[13,14] alkyl groups) that influence packing interactions and assembly motifs.

Although strategies towards 2- and 3-dimensional networks are currently being developed using ditopic 4,2′:6′,4″-tpy and its isomeric 3,2′:6′,3″-tpy linkers,[15,16] the coordination chemistry of 4,2′:6′,4″-tpy remains dominated by 1-dimensional chains. This preference can be modified by turning attention to the metal node. For example, linear $\{Zn_2(OAc)_4\}$ nodes (Scheme 1) combined with 4,2′:6′,4″-tpys

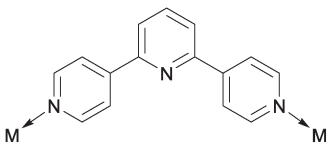

Scheme 1 Typical coordination mode of 4,2′:6′,4″-terpyridine.

Department of Chemistry, University of Basel, Spitalstrasse 51, CH-4056 Basel, Switzerland. E-mail: catherine.housecroft@unibas.ch

† Electronic supplementary information (ESI) available: Fig. S1–S5: powder diffraction data; Fig. S6: part of the coordination polymer chain in $[Cd_2(NO_3)_4(MeOH)(\mathbf{4})_3]_n$. CCDC 1402482–1402486. For ESI and crystallographic data in CIF or other electronic format see DOI: 10.1039/c2dt12242a

result in flat, zig-zag chains, whereas non-linear nodes (often incorporating zinc(II) halides) lead to helical polymers.[10] Single chains can be extended into double-stranded chains[17] by the use of $\{Cd_2(OAc)_4\}$ nodes which are structurally distinct from their zinc(II) counterparts (Scheme 2). This design principle is extended using $\{Mn_3(OAc)_6\}$ nodes for the assembly of triple-stranded chains,[18] but unexpectedly, planar $\{Zn_5(OAc)_{10}\}$ nodes lead to quadruple-stranded, rather than pentuple, chains.[19] Double chains in this family possess a ladder topology, with the rungs of the ladder defined by the $\{Cd_2(OAc)_4\}$-bridges (Scheme 2). The bridging mode of the acetato ligand is key to the formation of $\{M_n(OAc)_{2n}\}$ nodes, and the use of $[AcO]^-$ to assist the formation of multimetal, in particular zinc, cluster building blocks is well established with $[Zn_4(\mu\text{-}OAc)_6(\mu_4\text{-}O)]$[20] derivatives being fundamental to many metal organic frameworks (MOFs).[21]

Within the coordination chemistry of 4,2′:6′,4″-terpyridines, a switch from cadmium(II) acetate to nitrate significantly influences the coordination polymer assembly. For example, 4′-phenyl-4,2′:6′,4″-tpy reacts with $Cd(NO_3)_2{\cdot}4H_2O$ to give a 2-dimensional (4,4) net,[22] while introducing 4-$MeOC_6H_4$,[23] 4-$MeSC_6H_4$ [24] or 4-$HC{\equiv}CC_6H_4$ [24] units into the 4′-position of 4,2′:6′,4-tpy results in ladder assemblies in which each rung is defined by a 4,2′:6′,4″-tpy ligand. However, these ladders with a 2:3 ratio of Cd:ligand have been produced using different ratios of precursors in the crystallization experiments. We present here a systematic investigation of reactions of 4′-(4-alkoxyphenyl)-4,2′:6′,4″-terpyridines (Scheme 3) with cadmium(II) nitrate under room temperature conditions of crystallization. Our focus is to use a constant input ratio of $Cd(NO_3)_2{\cdot}4H_2O$ to ligand (1:3) in order to determine preferred assemblies and their reproducibility. We then demonstrate the effects of reducing the amount of ligand (Cd:ligand = 1:1) on the assembly process.

Experimental

Ligands **1**–**5** were prepared as previously described.[14]

$[\{Cd_2(NO_3)_4(2)_3\}{\cdot}3CHCl_3]_n$. A MeOH (8 mL) solution of $Cd(NO_3)_2{\cdot}4H_2O$ (9.25 mg, 0.03 mmol) was layered over a $CHCl_3$ (5 mL) solution of **2** (33.1 mg, 0.09 mmol) and the crystallization tube was left to stand at room temperature. Colourless crystals of $[\{Cd_2(NO_3)_4(2)_3\}{\cdot}3CHCl_3]_n$ (21.2 mg, 0.011 mmol, 73% based on Cd) were obtained after 2–4 weeks. Satisfactory elemental analysis of the bulk sample could not be obtained; see Fig. S1† for powder diffraction data.

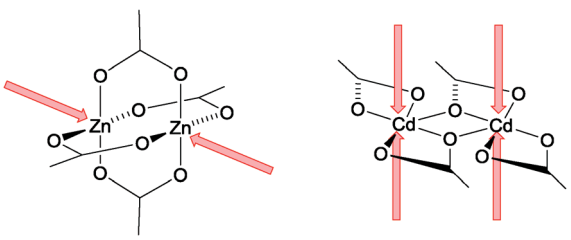

Scheme 2 Structurally different $\{Zn_2(OAc)_4\}$ and $\{Cd_2(OAc)_4\}$ nodes combine with 4,2′:6′,4″-tpy to give single and double-stranded chains, respectively.

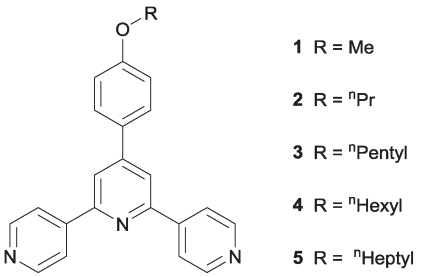

Scheme 3 Structures of ligands **1**–**5**.

$[\{Cd_2(NO_3)_4(3)_4\}{\cdot}3CHCl_3]_n$. A MeOH (8 mL) solution of $Cd(NO_3)_2{\cdot}4H_2O$ (3.08 mg, 0.01 mmol) was layered over a $CHCl_3$ (5 mL) solution of **3** (11.9 mg, 0.03 mmol) and the crystallization tube was left to stand at room temperature. Colourless crystals of $[\{Cd_2(NO_3)_4(3)_4\}{\cdot}3CHCl_3]_n$ (8.3 mg, 0.003 mmol, 69% based on Cd) were obtained after 2–4 weeks. Satisfactory elemental analysis of the bulk sample could not be obtained; see Fig. S2† for powder diffraction data.

$[\{Cd_2(NO_3)_4(4)_4\}{\cdot}CHCl_3{\cdot}MeOH]_n$. A MeOH (8 mL) solution of $Cd(NO_3)_2{\cdot}4H_2O$ (3.08 mg, 0.01 mmol) was layered over a $CHCl_3$ (5 mL) solution of **4** (12.4 mg, 0.03 mmol) and the crystallization was left to stand at room temperature. Colourless crystals of $[\{Cd_2(NO_3)_4(4)_4\}{\cdot}CHCl_3{\cdot}MeOH]_n$ (7.6 mg, 0.003 mmol, 67% based on Cd) were obtained after 2–4 weeks. Satisfactory elemental analysis of the bulk sample could not be obtained; see Fig. S3† for powder diffraction data.

$[\{Cd(NO_3)_2(5)_2\}{\cdot}2MeOH]_n$. A MeOH (8 mL) solution of $Cd(NO_3)_2{\cdot}4H_2O$ (3.08 mg, 0.01 mmol) was layered over a $CHCl_3$ (5 mL) solution of **5** (12.7 mg, 0.03 mmol) and the crystallization tube was left standing at room temperature. After 2–4 weeks, colourless crystals of $[\{Cd(NO_3)_2(5)_2\}{\cdot}2MeOH]_n$ (5.9 mg, 0.005 mmol, 51% based on Cd) had grown. Satisfactory elemental analysis of the bulk sample could not be obtained; see Fig. S4† for powder diffraction data.

$[Cd_2(NO_3)_4(MeOH)(4)_3]_n$. A MeOH (8 mL) solution of $Cd(NO_3)_2{\cdot}4H_2O$ (9.25 mg, 0.03 mmol) was layered over a $CHCl_3$ (5 mL) solution of **4** (12.4 mg, 0.03 mmol). The crystallization tube was left to stand at room temperature and colourless crystals of $[Cd_2(NO_3)_4(MeOH)(4)_3]_n$ (12.4 mg, 0.007 mmol, 48% based on Cd) were obtained after 2–4 weeks. Found C 56.11, H 5.07, N 10.83; required for $C_{82}H_{85}Cd_2N_{13}O_{16}$. MeOH C 56.47, H 5.08, N 10.31; see Fig. S5† for powder diffraction data.

Crystallography

Crystallographic data were collected on a Bruker-Nonius Kappa APEX diffractometer; data reduction, solution and refinement used APEX2[25] and CRYSTALS.[26] Powder

diffraction data were collected on a Stoe Stadi P powder diffractometer. Structural diagrams and structural analysis were carried out using Mercury v. 3.5.1,[27,28] and TOPOS.[29] The solvent region of three of the structures treated with the program SQUEEZE,[30] and the electron density removed was equated to appropriate solvent molecules and added to relevant formulae (see below). High thermal motion in some of the alkyl chains meant that some carbon atoms had to be refined isotropically; some bond parameters in these chains were restrained to chemically reasonable values.

$[\{Cd_2(NO_3)_4(2)_3\}\cdot 3CHCl_3]_n$. SQUEEZE[30] was used to treat the solvent region. $C_{75}H_{66}Cd_2Cl_9N_{13}O_{15}$, M = 1933.30, colourless block, monoclinic, space group $P2_1/n$, a = 15.0312(9), b = 25.4508(11), c = 21.7048(12) Å, β = 92.051(4)°, U = 8298.0(5) Å^3, Z = 4, D_c = 1.55 Mg m^{-3}, μ(Cu-Kα) = 7.363 mm^{-1}, T = 123 K. Total 55 690 reflections, 14 425 unique, R_{int} = 0.090. Refinement of 14 419 reflections (854 parameters) with $I > 2\sigma(I)$ converged at final R_1 = 0.0814 (R_1 all data = 0.1228), wR_2 = 0.2242 (wR_2 all data = 0.2753), gof = 0.9871. CCDC 1402483.

$[\{Cd_2(NO_3)_4(3)_4\}\cdot 3CHCl_3]_n$. SQUEEZE[30] was used to treat the solvent region. $C_{107}H_{103}Cd_2Cl_9N_{16}O_{16}$, M = 2412.97, colourless block, monoclinic, space group $P2_1/c$, a = 25.945(6), b = 24.578(5), c = 17.527(3) Å, β = 91.069(9)°, U = 11 174.7(17) Å^3, Z = 4, D_c = 1.43 Mg m^{-3}, μ(Cu-Kα) = 5.601 mm^{-1}, T = 123 K. Total 76 477 reflections, 19 048 unique, R_{int} = 0.047. Refinement of 19 027 reflections (1232 parameters) with $I > 2\sigma(I)$ converged at final R_1 = 0.1340 (R_1 all data = 0.1419), wR_2 = 0.3465 (wR_2 all data = 0.3513), gof = 1.0024. CCDC 1402485.

$[\{Cd_2(NO_3)_4(4)_4\}\cdot CHCl_3\cdot MeOH]_n$. SQUEEZE[30] was used to treat the solvent region. $C_{108}H_{112}Cd_2Cl_3N_{16}O_{17}$, M = 2261.35, colourless block, monoclinic, space group $P2_1/c$, a = 25.2624(12), b = 25.0809(11), c = 16.7959(8) Å, β = 92.522(3)°, U = 10 631.6(9) Å^3, Z = 4, D_c = 1.41 Mg m^{-3}, μ(Cu-Kα) = 4.500 mm^{-1}, T = 123 K. Total 44 477 reflections, 18 427 unique, R_{int} = 0.089. Refinement of 11 009 reflections (1191 parameters) with $I > 2\sigma(I)$ converged at final R_1 = 0.1026 (R_1 all data = 0.1279), wR_2 = 0.2838 (wR_2 all data = 0.3071), gof = 1.0024. CCDC 1402486.

$[\{Cd(NO_3)_2(5)_2\}\cdot 2MeOH]_n$. $C_{58}H_{66}CdN_8O_{10}$, M = 1147.61, colourless block, monoclinic, space group $P2_1/n$, a = 17.336(3), b = 17.302(3), c = 18.817(3) Å, β = 97.458(7)°, U = 5596.3(8) Å^3, Z = 4, D_c = 1.362 Mg m^{-3}, μ(Cu-Kα) = 3.658 mm^{-1}, T = 123 K. Total 11 3924 reflections, 9826 unique, R_{int} = 0.087. Refinement of 5855 reflections (659 parameters) with $I > 2\sigma(I)$ converged at final R_1 = 0.0986 (R_1 all data = 0.1359), wR_2 = 0.2752 (wR_2 all data = 0.3369), gof = 0.9707. CCDC 1402484.

$[Cd_2(NO_3)_4(MeOH)(4)_3]_n$. $C_{82}H_{85}Cd_2N_{13}O_{16}$, M = 1733.45, colourless block, triclinic, space group $P\bar{1}$, a = 13.1304(7), b = 16.5224(9), c = 19.2845(10) Å, α = 83.670(3), β = 82.840(3), γ = 70.242(3)°, U = 3896.3(2) Å^3, Z = 2, D_c = 1.477 Mg m^{-3}, μ(Cu-Kα) = 5.007 mm^{-1}, T = 123 K. Total 49 970 reflections, 13 661 unique, R_{int} = 0.039. Refinement of 12 221 reflections (1018 parameters) with $I > 2\sigma(I)$ converged at final R_1 = 0.0540 (R_1 all data = 0.0586), wR_2 = 0.1212 (wR_2 all data = 0.1228), gof = 0.9870. CCDC 1402482.

Photoluminescence. Solid-state quantum yields were measured using a Hamamatsu absolute PL quantum yield spectrometer C11347 Quantaurus_QY. Lifetimes and emission spectra of solid samples were measured using a Hamamatsu Compact Fluorescence lifetime Spectrometer C11367 Quantaurus-Tau; an LED light source with excitation wavelength of 280 nm was used.

Results and discussion

n-Propoxy-tailed 4,2′:6′,4″-terpyridine

We recently reported that under crystallization conditions in MeOH/$CHCl_3$, ligand **1** (Scheme 3) reacts with $Cd(NO_3)_2\cdot 4H_2O$ to give a 1-dimensional coordination ladder $[\{Cd_2(NO_3)_4(\mathbf{1})_3\}\cdot CHCl_3\cdot MeOH]_n$.[23] The ladder possesses a Cd : ligand ratio of 2 : 3, and both the rungs and rails of the ladder are defined by bridging ligands (Fig. 1). In order to probe the effects of lengthening the alkoxy chain in the linker, crystallization experiments combining $Cd(NO_3)_2\cdot 4H_2O$ with ligands **2**, **3**, **4** or **5** with ratios of Cd : ligand of 1 : 3 in MeOH/$CHCl_3$ were conducted. These resulted in the growth of X-ray quality crystals.

Structural analysis of a crystal selected from the bulk sample of crystals grown from the reaction of **2** (*n*-propoxy-tailed ligand) and $Cd(NO_3)_2\cdot 4H_2O$ confirmed the formation of $[\{Cd_2(NO_3)_4(2)_3\}\cdot 3CHCl_3]_n$. Cell checks on other crystals from the batch revealed consistent cell parameters. A comparison of the powder diffraction pattern for a batch of ground crystals from the bulk sample, with that of predicted from the single crystal structure is shown in Fig. S1.† The data are consistent with the single crystal being representative of the bulk sample.

$[\{Cd_2(NO_3)_4(2)_3\}\cdot 3CHCl_3]_n$ crystallizes in the monoclinic space group $P2_1/n$, and the asymmetric unit contains two independent Cd atoms and three independent ligands (Fig. 2). Although the Cd : ligand ratio of 2 : 3 is the same as in the coordination ladder $[\{Cd_2(NO_3)_4(\mathbf{1})_3\}\cdot CHCl_3\cdot MeOH]_n$, propagation of the structure in $[\{Cd_2(NO_3)_4(2)_3\}\cdot 3CHCl_3]_n$ leads to a 2-dimensional (6,3) net which lies in the *bc*-plane. Each of Cd1 and Cd2 is 7-coordinate, and is bound by the outer pyridine ring of three different ligands **2** and two bidentate nitrato ligands. Bond lengths are unexceptional (see caption to Fig. 2) and the bite angles of the four independent nitrato ligands are in the range 51.1(3)–52.2(3)°. The three N-donors at each Cd centre define a T-shaped environment with N–Cd–

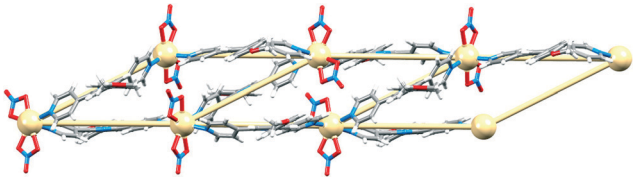

Fig. 1 Superimposition of the structure and TOPOS representation of part of one ladder in $[\{Cd_2(\mathbf{1})_3(NO_3)_4\}\cdot CHCl_3\cdot MeOH]_n$.[23]

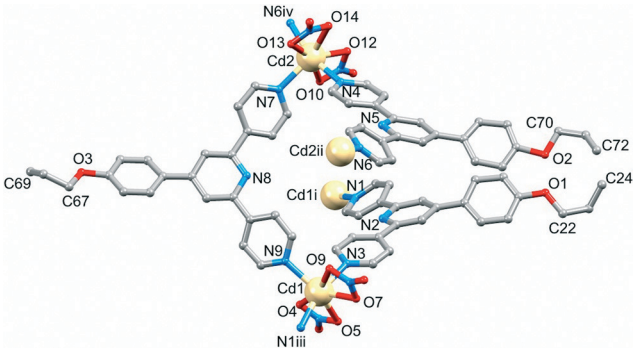

Fig. 2 The asymmetric unit (with symmetry generated atoms) in $[\{Cd_2(NO_3)_4(\mathbf{2})_3\}\cdot 3CHCl_3]_n$; H atoms omitted. Symmetry codes: i = 1/2 − *x*, 1/2 + *y*, 3/2 − *z*; ii = 1/2 − *x*, −1/2 + *y*, 1/2 − *z*; iii = 1/2 − *x*, −1/2 + *y*, 3/2 − *z*; iv = 1/2 − *x*, 1/2 + *y*, 1/2 − *z*. Selected bond distances: Cd1–O4 = 2.400(7), Cd1–O5 = 2.467(7), Cd1–O7 = 2.394(7), Cd1–O9 = 2.489(7), Cd1–N1^{iii} = 2.314(8), Cd1–N3 = 2.338(8), Cd1–N9 = 2.333(8), Cd2–O10 = 2.447(9), Cd2–O12 = 2.408(8), Cd2–O13 = 2.405(7), Cd2–O14 = 2.521(8), Cd2–N4 = 2.325(10), Cd2–N6 = 2.295(9), Cd2–N7 = 2.341(8) Å.

N angles (N1^{iii}–Cd1–N9 = 103.5(3) and N3–Cd1–N9 = 91.7(3)°, N6^{iv}–Cd2–N7 = 104.7(3) and N4–Cd2–N7 = 91.6(3)°).

Around each 6-membered ring in the (6,3) net, the bridging ligands with extended chains are in an up/up/down/up/up/down sequence, and the nets stack over one another in an ABAB··· arrangement with A and B layers related by inversion (Fig. 3a). The closest Cd···Cd separation between nets is 7.836(1) Å, which is significantly shorter that the separations of 12.3597(9) to 12.9881(9) Å within each hexacycle in the (6,3) net; the latter distances are imposed by the span of bridging ligand **2**. Fig. 3b illustrates the penetration of the 4-propoxyphenyl groups through adjacent sheets. The chain containing atom O3 is neatly accommodated (Fig. 4) within a pocket comprising three ligands **2** containing N3^{v}, N5^{v} and N8^{v} (symmetry code v = 1 + *x*, *y*, *z*). The pyridine ring with N8 is sandwiched between two phenyl rings in adjacent chains; angles between the least squares planes of the rings in the triple π-stack (Fig. 4) are 7.9 and 6.2°, and the $\text{phenyl}_{\text{centroid}}\cdots\text{pyridine}_{\text{plane}}$ distances are 3.54 and 3.53 Å. The close H···H contacts highlighted in green in Fig. 4 are an important feature of this 'tail-in-pocket' interaction, and limit the length of the alkyl chain that can be accommodated. We were able to obtain preliminary structural data on crystals grown from the reaction of $Cd(NO_3)_2\cdot 4H_2O$ and 4′-(4-*n*-butoxyphenyl)-4,2′:6′,4″-tpy. Significantly, the cell dimensions (*a* = 15.241(9), *b* = 25.2808(13), *c* = 21.913(2) Å, *β* = 90.75(4)°) are similar to those of $[\{Cd_2(NO_3)_4(\mathbf{2})_3\}\cdot 3CHCl_3]_n$ and the preliminary determination confirmed the assembly of a (6,3) with analogous structural features to those shown in Fig. 3 and 4. This implies that no major structural perturbation occurs on going from an *n*-propoxy to *n*-butoxy functionalized ligand.

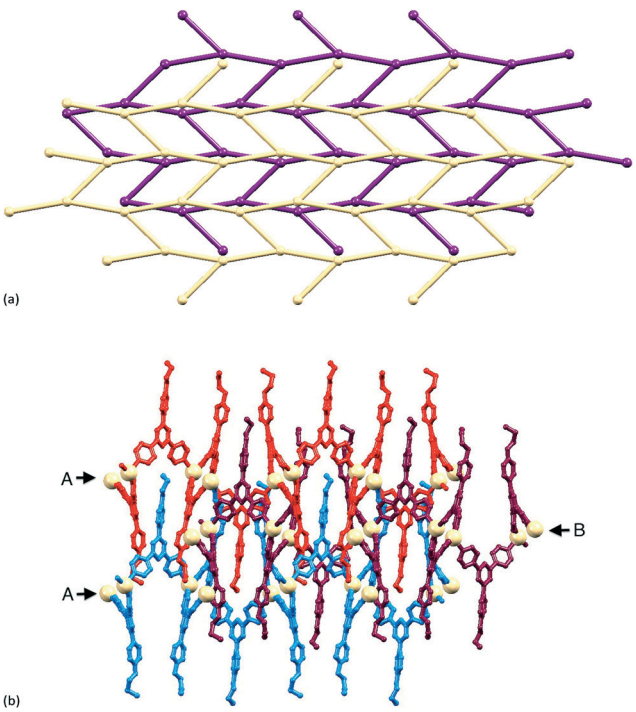

Fig. 3 Structure of $[\{Cd_2(NO_3)_4(\mathbf{2})_3\}\cdot 3CHCl_3]_n$: (a) TOPOS representation of adjacent (6,3) nets (viewed down the *a*-axis); (b) part of three sheets (ABA arrangement) showing the penetration of 4-propoxyphenyl units through adjacent sheets.

From *n*-propoxy to *n*-pentoxy and *n*-hexoxy tails

Reaction of $Cd(NO_3)_2\cdot 4H_2O$ with **3** or **4** (*n*-pentoxy or *n*-hexoxy derivatives, Scheme 3) leads to $[\{Cd_2(NO_3)_4(\mathbf{3})_4\}\cdot 3CHCl_3]_n$ or $[\{Cd_2(NO_3)_4(\mathbf{4})_4\}\cdot CHCl_3\cdot MeOH]_n$, respectively. The compounds are structurally analogous, crystallizing in the space group $P2_1/c$ with similar cell dimensions. Cell parameters consistent with those in the experimental section for $[\{Cd_2(NO_3)_4(\mathbf{3})_4\}\cdot 3CHCl_3]_n$ and $[\{Cd_2(NO_3)_4(\mathbf{4})_4\}\cdot CHCl_3\cdot MeOH]_n$ were obtained for represenative crystals chosen from the bulk sample. Fig. S2 and S3† compare the powder diffraction patterns predicted from the single crystal structures of the two coordination polymers with those of ground crystals from the bulk material, and with experimental powder patterns for the precursors. The data confirm that the single crystals chosen were representative of the bulk samples.

In the light of the restricted space associated with the 'tail-in-pocket' interaction in $[\{Cd_2(NO_3)_4(\mathbf{2})_3\}\cdot 3CHCl_3]_n$ and its *n*-butoxy analogue, a change in structure on going to the

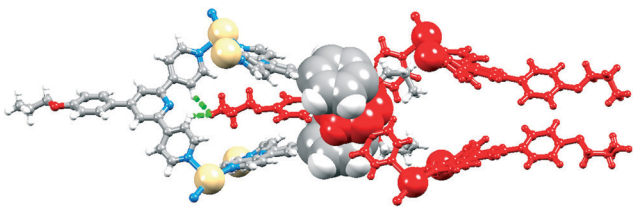

Fig. 4 Accommodation of the 4-propoxyphenyl unit (red) containing atom O3 in a pocket comprising three ligands **2**; short H···H contacts (2.14 and 2.49 Å) are shown in green. See text for details of the π-stacking interaction.

longer *n*-pentoxy or *n*-hexoxy chains is not unexpected. Fig. 5 shows the asymmetric unit (with symmetry generated atoms) in $[\{Cd_2(NO_3)_4(\mathbf{4})_4\}\cdot CHCl_3\cdot MeOH]_n$, with two independent Cd atoms and four independent ligands **4**. Likewise, $[\{Cd_2(NO_3)_4(\mathbf{3})_4\}\cdot 3CHCl_3]_n$ contains two independent Cd atoms and four independent molecules of **3**. The Cd atoms are octahedrally sited, coordinated by four ligands and two, mutually *trans* nitrato ligands. The Cd–N bond lengths are in the range 2.317(9) to 2.362(8) Å in $[\{Cd_2(NO_3)_4(\mathbf{3})_4\}\cdot 3CHCl_3]_n$, and 2.286(8) to 2.407(4) Å in $[\{Cd_2(NO_3)_4(\mathbf{4})_4\}\cdot CHCl_3\cdot MeOH]_n$. The coordination modes of the nitrato ligands in the two compounds are monodentate, bidentate (Fig. 5) or monodentate with an additional long contact; Cd–O distances range from 2.360(7) to 2.879(9) Å in $[\{Cd_2(NO_3)_4(\mathbf{3})_4\}\cdot 3CHCl_3]_n$ and from 2.310(12) to 2.616(8) Å in $[\{Cd_2(NO_3)_4(\mathbf{4})_4\}\cdot CHCl_3\cdot MeOH]_n$. In each structure, one nitrato ligand is disordered and has been modelled over two sites with fractional occupancies of 0.60/0.40 or 0.65/0.35. Each Cd atom in $[\{Cd_2(NO_3)_4(\mathbf{3})_4\}\cdot 3CHCl_3]_n$ and $[\{Cd_2(NO_3)_4(\mathbf{4})_4\}\cdot CHCl_3\cdot MeOH]_n$ acts as a 4-connecting node giving the (4,4) coordination networks shown in Fig. 6 and 7. Each rhombus in the net in $[\{Cd_2(NO_3)_4(\mathbf{3})_4\}\cdot 3CHCl_3]_n$ (Fig. 6a) is characterized by Cd···Cd distances in a range 12.502(3) to 13.063(3) Å and internal angles of 79.02(1), 99.89(1), 79.91(1) and 101.19(1)°. In the net in $[\{Cd_2(NO_3)_4(\mathbf{4})_4\}\cdot CHCl_3\cdot MeOH]_n$ (Fig. 7), each rhombus has Cd···Cd distances between 12.4678(9) and 12.771(1) Å and internal angles of 86.26(1), 92.31(1), 87.61(1) and 93.82(1)°. The bridging ligands **3** or **4** linking the Cd nodes project above and below the net (Fig. 6b), and adopt an up/up/up/down arrangement working around the four sides of the rhombus.

In $[\{Cd_2(NO_3)_4(\mathbf{3})_4\}\cdot 3CHCl_3]_n$ and $[\{Cd_2(NO_3)_4(\mathbf{4})_4\}\cdot CHCl_3\cdot MeOH]_n$, the (4,4) nets lie parallel to the *ab*-plane. The alkoxy chains are in extended or close to extended conformations and are directed approximately along the *c*-axis (Fig. 6b). This has the effect of locking the nets with the 4-membered macrocycles almost directly over one another as shown in Fig. 8 for $[\{Cd_2(NO_3)_4(\mathbf{3})_4\}\cdot 3CHCl_3]_n$. Pairs of pyridine rings (containing N2 and N5^{iv}, symmetry code iv = x, 1/2 − y, −1/2 + z) in ligands from adjacent sheets engage in efficient face-to-face π-stacking interactions; the angle between the least squares planes of the rings is 1.5° and ring-plane to centroid separation = 3.38 Å. (These parameters for the analogous interactions in $[\{Cd_2(NO_3)_4(\mathbf{4})_4\}\cdot CHCl_3\cdot MeOH]_n$ are 0.4° and 3.49 Å.) These interactions (two per macrocycle, Fig. 8b) are central to interlocking the sheets. The shortest Cd···Cd separations between sheets are 8.940(2) and 8.894(2) Å in $[\{Cd_2(NO_3)_4(\mathbf{3})_4\}\cdot 3CHCl_3]_n$, and 8.468(1) and 8.433(1) Å in $[\{Cd_2(NO_3)_4(\mathbf{4})_4\}\cdot CHCl_3\cdot MeOH]_n$; this places the 4′-phenyl substituents of ligands **3** or **4** within the (4,4) net defined by the Cd atoms (central part of Fig. 8a). Additional voids in the lattice are occupied by solvent molecules. SQUEEZE[30] was used to treat the solvent region; the rationalized solvent content in the structurally similar coordination networks in $[\{Cd_2(NO_3)_4(\mathbf{3})_4\}\cdot 3CHCl_3]_n$ and $[\{Cd_2(NO_3)_4(\mathbf{4})_4\}\cdot CHCl_3\cdot MeOH]_n$ is consistent with the greater spatial demands of ligand **4** *versus* **3**.

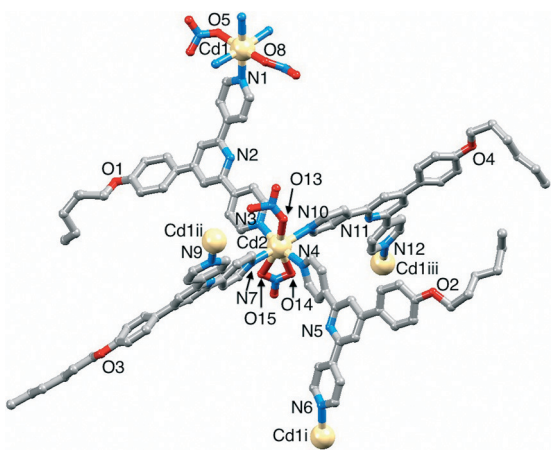

Fig. 5 The asymmetric unit (with symmetry generated atoms) in $[\{Cd_2(NO_3)_4(\mathbf{4})_4\}\cdot CHCl_3\cdot MeOH]_n$; H atoms and solvent molecules omitted. Symmetry codes: i = 1 + x, y, z; ii = 2 − x, −1/2 + y, 3/2 − z; iii = 2 − x, 1/2 + y, 3/2 − z.

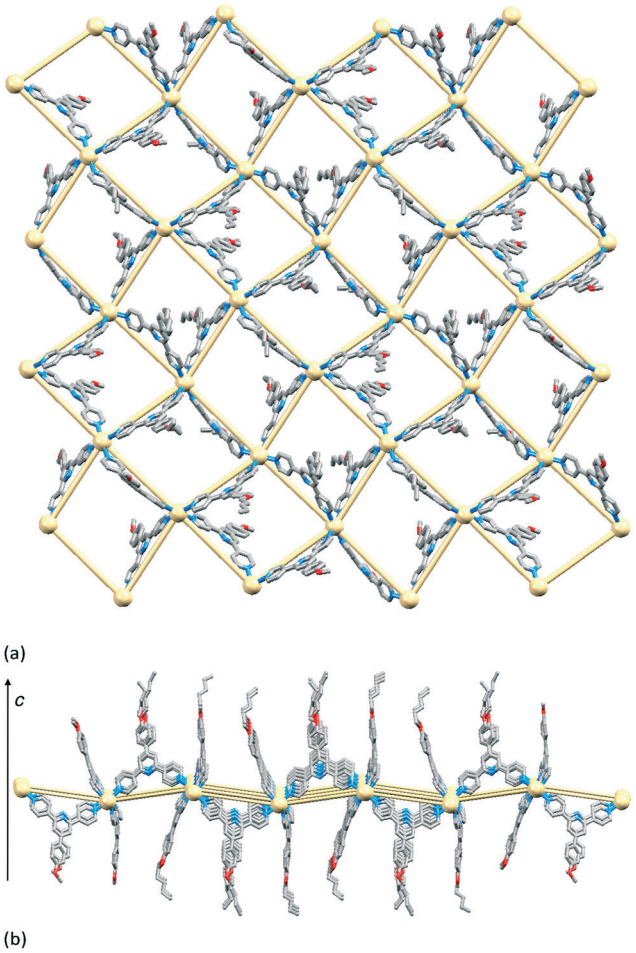

Fig. 6 (a) Superimposition of the structure and TOPOS representation of part of the (4,4) net in $[\{Cd_2(NO_3)_4(\mathbf{3})_4\}\cdot 3CHCl_3]_n$ viewed down the *c*-axis. (b) View down the *a*-axis showing projection of the ligands above and below the sheet. Nitrato ligands, H atoms and solvent molecules omitted.

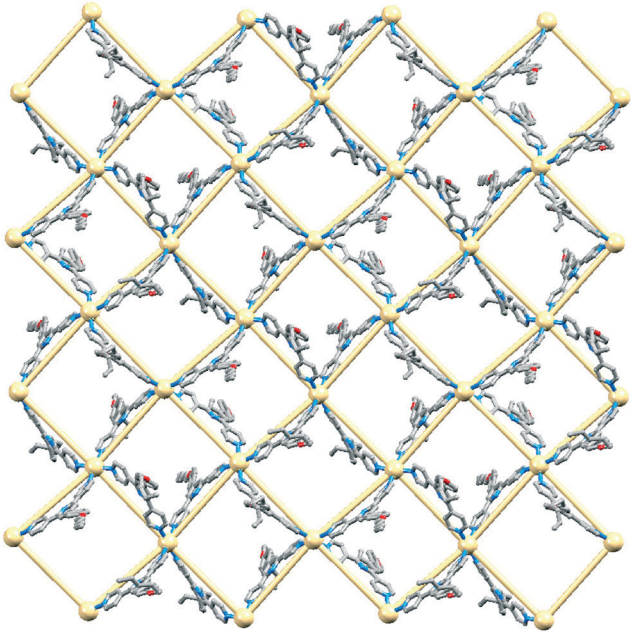

Fig. 7 Superimposition of the structure and TOPOS representation of part of the (4,4) net in $[\{Cd_2(NO_3)_4(\mathbf{4})_4\}\cdot CHCl_3\cdot MeOH]_n$ viewed down the *c*-axis. Nitrato ligands, H atoms and solvent molecules omitted.

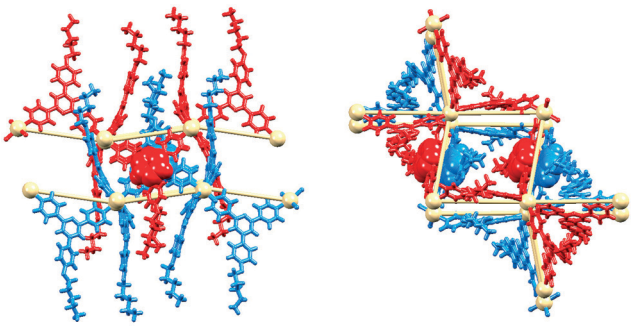

(a) (b)

Fig. 8 $[\{Cd_2(NO_3)_4(\mathbf{3})_4\}\cdot 3CHCl_3]_n$: (a) view down the *a*-axis of part of two sheets (red and blue, Cd atoms and net in TOPOS representation) showing π-stacking between two 4,2′:6′,4″-tpy domains in space filling representation; (b) the same unit viewed down the *c*-axis showing approximate superimposition of 4-membered macrocycles in adjacent nets.

n-Hexoxy to *n*-heptoxy tails and a switch from *trans*- to *cis*-coordination

The effects of further chain lengthening were investigated by treating $Cd(NO_3)_2\cdot 4H_2O$ with ligand **5** which contains an *n*-heptoxy tail (Scheme 3). X-ray quality crystals grown under the same conditions as those with ligands **2**–**4** proved to be $[\{Cd(NO_3)_2(\mathbf{5})_2\}\cdot 2MeOH]_n$. The powder diffraction data shown in Fig. S4† are consistent with the single crystal being representative of the bulk sample.

As in the (4,4) networks with ligands **3** and **4**, the Cd atom in $[\{Cd(NO_3)_2(\mathbf{5})_2\}\cdot 2MeOH]_n$ is octahedrally sited and is coordinated by four 4,2′:6′,4″-tpy and two nitrato ligands. However, the nitrato groups are mutually *cis* (Fig. 9a), in contrast to *trans*-arrangements in $[\{Cd_2(NO_3)_4(\mathbf{3})_4\}\cdot 3CHCl_3]_n$ and $[\{Cd_2(NO_3)_4(\mathbf{4})_4\}\cdot CHCl_3\cdot MeOH]_n$. Bond parameters for the coordination sphere are given in the caption to Fig. 9a. The alkoxy chain with O1 is in a fully extended conformation while that with O2 is folded out of the plane of the phenyl ring to which it is bonded. The Cd atoms act as 4-connecting nodes and assemble into a (4,4) net. Compared to the up/up/up/down arrangement of bridging ligands around each 4-membered metallomacrocycle in $[\{Cd_2(NO_3)_4(\mathbf{3})_4\}\cdot 3CHCl_3]_n$ and $[\{Cd_2(NO_3)_4(\mathbf{4})_4\}\cdot CHCl_3\cdot MeOH]_n$, those in $[\{Cd(NO_3)_2(\mathbf{5})_2\}\cdot 2MeOH]_n$ adopt an up/down/up/down arrangement (Fig. 9b). The two independent Cd···Cd distances within the (4,4) net are 12.938(2) and 12.630(2) Å. The Cd nodes in each net lie in a plane (deviation is ±0.1 Å); the sheets stack over one another (Fig. 10a) and the shortest Cd···Cd separations are 8.566(2) and 8.950(2) Å.

Fig. 10b shows a superimposition of the structure and TOPOS representation of part of one (4,4) net in $[\{Cd(NO_3)_2(\mathbf{5})_2\}\cdot 2MeOH]_n$. A comparison of this with Fig. 6a and 7 illustrates that both *cis* and *trans*-arrangements of nitrato ligands lead to cavities in the network through which long alkoxy chains from the next sheet can penetrate. This is shown for $[\{Cd(NO_3)_2(\mathbf{5})_2\}\cdot 2MeOH]_n$ in Fig. 11a. Just as in $[\{Cd_2(NO_3)_4(\mathbf{3})_4\}\cdot 3CHCl_3]_n$ and $[\{Cd_2(NO_3)_4(\mathbf{4})_4\}\cdot CHCl_3\cdot MeOH]_n$, 4,2′:6′,4″-tpy domains in adjacent sheets interact through π-stacking of the central pyridine rings (Fig. 11b). The angle between the least squares planes of the rings containing N2 ad $N5^{i}$ (symmetry code i = 1 − *x*, 1 − *y*, 1 − *z*) is 5.4° and the ring-plane to centroid separation is 3.57 Å. This type of interaction is found in a range of coordination polymers involving 4,2′:6′,4″-tpy ligands.[10] Fig. 11b also shows that the depth of penetration of one sheet into the next is such that the 4-phenyl substituent in ligand **5** lies within the (4,4) net of Cd atoms. Again this mimics the situation in the networks involving ligands **3**

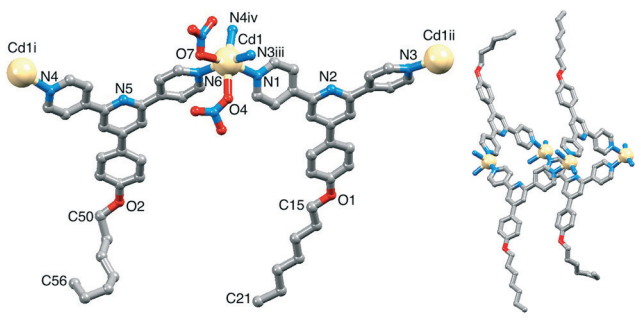

(a) (b)

Fig. 9 (a) The asymmetric unit (with symmetry generated atoms) in $[\{Cd(NO_3)_2(\mathbf{5})_2\}\cdot 2MeOH]_n$; H atoms and solvent molecules omitted. Symmetry codes: i = 1/2 − *x*, −1/2 + *y*, 1/2 − *z*; ii = 1/2 − *x*, 1/2 + *y*, 3/2 − *z*; iii = 1/2 − *x*, −1/2 + *y*, 3/2 − *z*; iv = 1/2 − *x*, 1/2 + *y*, 1/2 − *z*. Selected bond parameters: Cd1–O4 = 2.363(8), Cd1–O6 = 3.030(10), Cd1–O7 = 2.440(8), Cd1–N1 = 2.399(9), Cd1–$N3^{iii}$ = 2.317(8), Cd1–$N4^{iv}$ = 2.359(9), Cd1–N6 = 2.341(8) Å; O4–Cd1–O7 = 86.0(3); N1–Cd1–N6 = 98.7(3), O7–Cd1–N1 = 165.2(3), O4–Cd1–$N4^{iv}$ = 163.2(3)°. (b) One 4-membered metallomacrocyclic unit with up/down/up/down arrangement of ligands **5**.

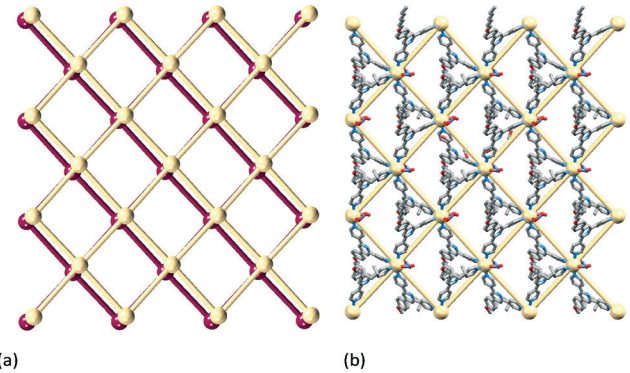

Fig. 10 Structure of $[\{Cd(NO_3)_2(\mathbf{5})_2\}\cdot 2MeOH]_n$ (viewed down the *a*-axis): (a) TOPOS representation of adjacent (4,4) nets; (b) superimposition of the structure and TOPOS representation of part of one (4,4) net; H atoms and solvent molecules omitted.

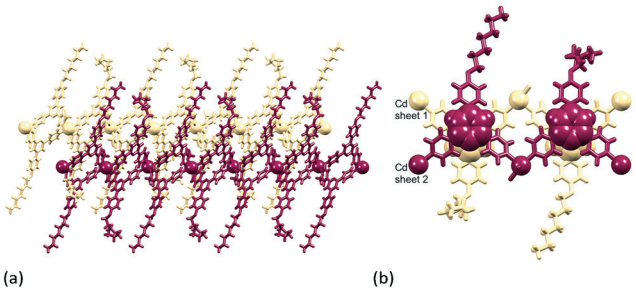

Fig. 11 (a) Penetration of 4-alkoxyphenyl units of one sheet through the 4-membered metallocycles of an adjacent sheet in $[\{Cd(NO_3)_2(\mathbf{5})_2\}\cdot 2MeOH]_n$. (b) π-stacking between two 4,2′:6′,4″-tpy domains (space filling representation) in adjacent sheets.

and **4**, and leads to a similar inter-sheet separation; shortest Cd···Cd distances between nets are 8.566(2) and 8.950(2) Å with ligand **5** *versus* 8.940(2) and 8.894(2) Å with **3**, and 8.468(1) and 8.433(1) Å with **4**. Thus, despite the change in the local environment at the Cd centre on going from a *trans*- to *cis*-ligand arrangement, the packing interactions between the sheets remain similar.

A change in the ratio of cadmium : ligand

For the coordination networks described above, the ratio of cadmium : ligand in the crystallization experiments was 1 : 3 leading to networks with a 2 : 3 ratio of Cd : ligand **2**, or 1 : 2 for ligands **3**, **4** or **5**. For the hexoxy-tailed ligand **4**, a crystallization experiment was also run with a 1 : 1 ratio of Cd : ligand. Structural analysis (see Fig. S5† for powder diffraction data) revealed the formation of the 1-dimensional coordination polymer $[Cd_2(NO_3)_4(MeOH)(\mathbf{4})_3]_n$ which crystallizes in the triclinic space group $P\bar{1}$, and possesses a ladder structure (Fig. 12 and S6†). The structure is similar to that found for $[\{Cd_2(NO_3)_4(\mathbf{1})_3\}\cdot CHCl_3\cdot MeOH]_n$.[23] The asymmetric unit contains two independent Cd atoms and three independent ligands **4**. Atom Cd1 is 8-coordinate (Fig. 12), binding to three 4,2′:6′,4″-tpys (Cd1–N1 = 2.316(3), Cd1–N4 = 2.359(4),

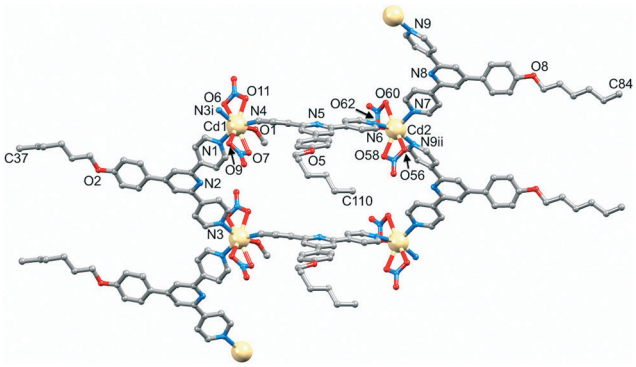

Fig. 12 Building block in the polymer chain in $[Cd_2(NO_3)_4(MeOH)(\mathbf{4})_3]_n$. Atoms in the asymmetric unit are labelled; symmetry codes: i = −1 + *x*, *y*, *z*; ii = 1 + *x*, *y*, *z*. Hydrogen atoms are omitted for clarity.

Cd1–$N3^i$ = 2.340(3) Å), an MeOH molecule (Cd1–O1 = 2.428(3) Å) and two bidentate nitrato ligands, although one Cd–O contact is long (Cd1–O6 = 2.754(4), Cd1–O7 = 2.518(4), Cd1–O9 = 2.541(4), Cd1–O11 = 2.421(3) Å). Atom Cd2 is 7-coordinate (Fig. 12), coordinated by three 4,2′:6′,4″-tpys (Cd2–$N9^{ii}$ = 2.313(4), Cd2–N6 = 2.347(3), Cd2–N7 = 2.302(4) Å) and two bidentate nitrato groups (Cd2–O56 = 2.458(3), Cd2–O58 = 2.455(4), Cd2–O60 = 2.626(4), Cd2–O62 = 2.361(3) Å). The three N-donors at each Cd centre are in a T-shaped arrangement (angles $N3^i$–Cd1–N1 = 104.91(12) and $N3^i$–Cd1–N4 = 93.72(13), $N9^{ii}$–Cd2–N7 = 103.53(13) and N6–Cd2–N7 = 92.16(13)°).

Although topologically the ladders in $[\{Cd_2(NO_3)_4(\mathbf{1})_3\}\cdot CHCl_3\cdot MeOH]_n$ and $[Cd_2(NO_3)_4(MeOH)(\mathbf{4})_3]_n$ are the same, the internal angles of each rhombus in the ladder as defined by the ligand-bridged Cd nodes are 82 and 98° in $[Cd_2(NO_3)_4(MeOH)(\mathbf{4})_3]_n$ (Fig. 13 and S6†), and 27.3 and 152.7° in $[\{Cd_2(NO_3)_4(\mathbf{1})_3\}\cdot CHCl_3\cdot MeOH]_n$ (Fig. 14). The rails (vertical in Fig. 13 and 14) of the ladder are slipped with respect to one another on going from **4** to **1**, and the closest Cd···Cd separation across the ladder decreases from 13.0025(8) Å (ligand-bridged) in

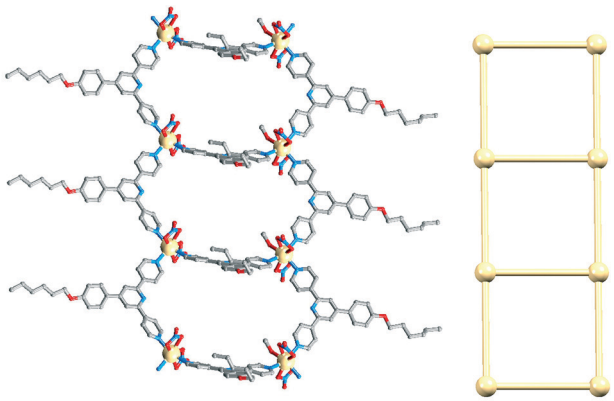

Fig. 13 (a) Part of the 1-dimensional coordination polymer in $[Cd_2(NO_3)_4(MeOH)(\mathbf{4})_3]_n$ and (b) TOPOS representation of part of the ladder.

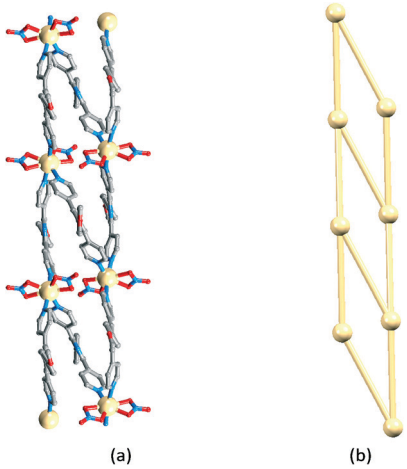

Fig. 14 (a) Part of the 1-dimensional coordination polymer in $[\{Cd_2(NO_3)_4(\mathbf{1})_3\}\cdot CHCl_3\cdot MeOH]_n$ and (b) TOPOS representation of part of a ladder.

$[Cd_2(NO_3)_4(MeOH)(\mathbf{4})_3]_n$ to 6.094(1) Å (unbridged) in $[\{Cd_2(NO_3)_4(\mathbf{1})_3\}\cdot CHCl_3\cdot MeOH]_n$.[23] The ladder conformation shown in Fig. 14b is also seen in $[\{Cd_2(NO_3)_4\ \mathbf{L}_3\}\cdot 4MeOH\cdot 2CHCl_3]_n$ and $[\{Cd_2(NO_3)_4\ \mathbf{L}_3\}\cdot 2MeOH\cdot 3CHCl_3\cdot H_2O]_n$ in which **L** = 4′-(4-MeSC$_6$H$_4$)-4,2′:6′,4″-tpy or 4′-(4-HC≡CC$_6$H$_4$)-4,2′:6′,4″-tpy.[24] A comparison of Fig. 13a and 14a reveals that the ligands defining the rails of the ladder in $[Cd_2(NO_3)_4(MeOH)(\mathbf{4})_3]_n$ (Fig. 13) point outwards from the ladder-framework, in contrast to their orientation in the ladder type found for $[\{Cd_2(NO_3)_4(\mathbf{1})_3\}\cdot CHCl_3\cdot MeOH]_n$ and its analogues.[23,24] Primary packing forces between adjacent coordination polymer chains involve both π-stacking and van der Waals interactions. Adjacent ladders in $[Cd_2(NO_3)_4(MeOH)(\mathbf{4})_3]_n$ interact through a centrosymmetric face-to-face π-stacking of the central pyridine rings of the ligands **4** forming the rungs of the ladder (Fig. 15); the distance between the N5- and N5^{iii}-containing ring planes (symmetry code iii = $-x$, $1-y$, $1-z$) is 3.39 Å and the inter-centroid separation is 3.55 Å. The alkoxy chains containing atoms O2 and O8 are in fully extended conformations and chains from adjacent ladders interdigitate with one another as shown in Fig. 15. The terminal methyl group of each 4-hexoxyphenyl unit lies over the arene ring of the next substituent giving a head-to-tail embrace; both independent $C_{Me}\cdots centroid_{arene}$ distances are 3.78 Å. Extension of the packing motif in Fig. 15 generates sheets which are locked together by penetration of the protruding, folded hexoxy chains into cavities in the next sheet.

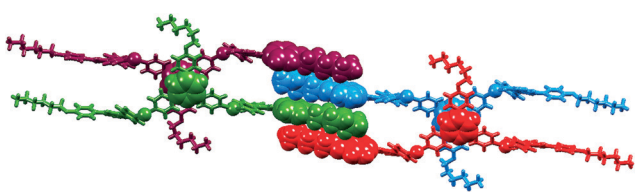

Fig. 15 Four ladders in $[Cd_2(NO_3)_4(MeOH)(\mathbf{4})_3]_n$ viewed down the *a*-axis showing π-stacking interactions and interdigitation between 4-hexoxyphenyl substituents between adjacent polymer chains.

Solid-state photoluminescence

Protonation of 2,2′:6′,2″-terpyridine (2,2′:6′,2″-tpy) significantly enhances the photoluminescence (PL) of the ligand in MeCN solution, leading to a red-shift in λ_{max}^{em} from 340 nm to 412 nm, and an increase in quantum yield (QY) from <0.1% to 5.2%.[31] Diprotonation results in a further increase in QY.[32] It has also been observed that in the solid state, amorphous 2,2′:6′,2″-tpy and needle-like crystals (melting point 86–88 °C) are non-emissive, while plate-like crystals (melting point 91–93 °C) are photoluminescent (λ_{max}^{em} = 365 nm) with QY = 20% and an emission lifetime of 4.5 ns.[33] The emission maxima (Fig. 16) and PL quantum yields of crystalline **2**–**4** are given in Table 1. All are blue emitters, with QY values ranging from 15 to 27%; the emission lifetimes are <10 ns. Incorporation of the alkoxy-substituent red-shifts the emission with respect to that of solid 4′-phenyl-4,2′:6′,4″-terpyridine; the latter emits weakly (λ_{max}^{em} = 370 nm) when excited at 345 nm.[34] Note that Hou and Li have reported that solid 4′-phenyl-4,2′:6′,4″-terpyridine exhibits a strong green PL (λ_{max}^{em} = 517 nm, λ_{exc} = 400 nm).[35]

Fig. 16 shows the emission spectra of solid samples of $[\{Cd_2(NO_3)_4(\mathbf{2})_3\}\cdot 3CHCl_3]_n$, $[\{Cd_2(NO_3)_4(\mathbf{3})_4\}\cdot 3CHCl_3]_n$ and $[\{Cd_2(NO_3)_4(\mathbf{4})_4\}\cdot CHCl_3\cdot MeOH]_n$ (all 2-dimensional networks) and of $[Cd_2(NO_3)_4(MeOH)(\mathbf{4})_3]_n$ (a 1-dimensional ladder). With the exception of $[\{Cd_2(NO_3)_4(\mathbf{4})_4\}\cdot CHCl_3\cdot MeOH]_n$, the emission broadens and shifts to lower energy on going from free ligand to complex, but remains in the blue region. Similar red-shifts have been reported when N-donor ligands coordinate to zinc(II) or cadmium(II), and the emissions are assigned to intra-ligand transitions.[34,36] On going from **4** to $[\{Cd_2(NO_3)_4(\mathbf{4})_4\}\cdot CHCl_3\cdot MeOH]_n$, the emission band broadens but λ_{em}^{max} remains at 420 nm. The formation of the coordination polymers incorporating **2**, **3** or **4** has little effect on the QYs compared to those of the free ligands, and for each complex, the emission lifetime is <10 ns.

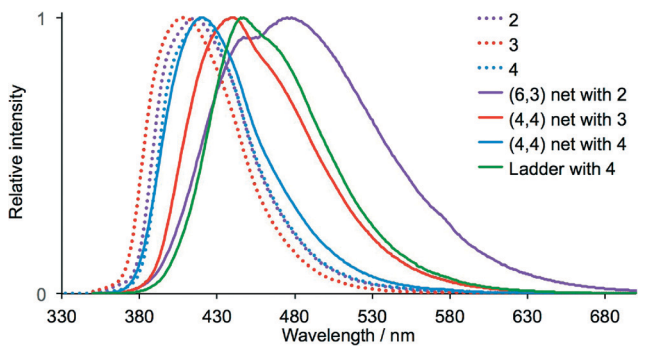

Fig. 16 Solid-state emission spectra of ligands **2**–**4** (dotted lines) and of the 2-dimensional coordination networks $[\{Cd_2(NO_3)_4(\mathbf{2})_3\}\cdot 3CHCl_3]_n$ (solid purple line), $[\{Cd_2(NO_3)_4(\mathbf{3})_4\}\cdot 3CHCl_3]_n$ (solid red line) and $[\{Cd_2(NO_3)_4(\mathbf{4})_4\}\cdot CHCl_3\cdot MeOH]_n$ (solid blue line), and of the 1-dimensional ladder $[Cd_2(NO_3)_4(MeOH)(\mathbf{4})_3]_n$ (green curve). (λ_{exc} = 280 nm).

Table 1 Photoluminescence of **2**–**4** and their coordination networks in the solid state

Compound	λ_{exc}/nm	λ_{em}^{max}/nm	QY/%
2	280	416	15
3	280	408	27
4	280	420	17
$[\{Cd_2(NO_3)_4(\mathbf{2})_3\}\cdot 3CHCl_3]_n$	280	475	11
$[\{Cd_2(NO_3)_4(\mathbf{3})_4\}\cdot 3CHCl_3]_n$	280	440	22
$[\{Cd_2(NO_3)_4(\mathbf{4})_4\}\cdot CHCl_3\cdot MeOH]_n$	280	420	13
$[Cd_2(NO_3)_4(MeOH)(\mathbf{4})_3]_n$	280	447	18

Conclusions

The divergent *N*,*N*-binding mode of 4,2′:6′,4″-terpyridines is readily exploited for the formation of coordination polymers and networks, but determining factors that can encourage the formation of 2- and 3-dimensional networks remains under-developed. In this work, we have demonstrated the structural consequences of increasing the length of the alkoxy substituent in 4′-alkoxy-4,2′:6′,4″-terpyridines when these ligands combine with $Cd(NO_3)_2\cdot 4H_2O$ with a Cd : ligand ratio of 1 : 3. Ligand **2** contains a 4′-*n*-propoxy substituent and forms $[\{Cd_2(NO_3)_4(\mathbf{2})_3\}\cdot 3CHCl_3]_n$ consisting of a (6,3) net. *n*-Propoxy chains protrude from the sheet and are involved in 'tail-in-pocket' interactions which interlock the sheets. Although preliminary data indicate that an *n*-butoxy chain causes no major structural perturbation, introduction of longer chains cause a switch from a (6,3) to (4,4) net. The change is consistent with the pockets in which the smaller chains are accommodated when (6,3) sheets pack together are too small to accommodate longer chains. In $[\{Cd_2(NO_3)_4(\mathbf{3})_4\}\cdot 3CHCl_3]_n$ and $[\{Cd_2(NO_3)_4(\mathbf{4})_4\}\cdot CHCl_3\cdot MeOH]_n$ each 4-connecting Cd atom has a *trans*-arrangement of nitrato ligands, while in $[\{Cd(NO_3)_2(\mathbf{5})_2\}\cdot 2MeOH]_n$, they are *cis*. The reaction between $Cd(NO_3)_2\cdot 4H_2O$ and **4** using a 1 : 1 ratio of Cd : ligand switches the assembly to a 1-dimensional ladder; in $[Cd_2(NO_3)_4(MeOH)(\mathbf{4})_3]_n$ each Cd atom is a 3-connecting node. Face-to-face π-interactions between arene rings (either pyridine/pyridine or pyridine/phenyl) in adjacent sheets or chains are a common feature of the coordination networks, and van der Waals interactions between *n*-hexoxy chains play a dominant role in the packing of ladders in $[Cd_2(NO_3)_4(MeOH)(\mathbf{4})_3]_n$. In the solid state, the coordination polymers are blue emitters; values of λ_{em}^{max} are red-shifted up to 59 nm with respect to the free ligand, and quantum yields are in the range 11–22%.

Acknowledgements

We thank the Swiss National Science Foundation, the European Research Council (Advanced Grant 267816 LiLo) and the University of Basel for financial support. The Swiss National Science Foundation through the NCCR Molecular Systems Engineering is acknowledged for partial funding of the powder diffractometer. Dr Collin D. Morris is thanked for assistance with powder diffraction and photoluminescence measurements.

Notes and references

1 P. J. Stang and B. Olenyuk, *Acc. Chem. Res.*, 1997, **30**, 502.
2 S. Leininger, B. Olenyuk and P. J. Stang, *Chem. Rev.*, 2000, **100**, 853.
3 S. R. Seidel and P. J. Stang, *Acc. Chem. Res.*, 2002, **35**, 972.
4 B. H. Northrop, H. B. Yang and P. J. Stang, *Chem. Commun.*, 2008, 5896.
5 M. Yoshizawa, J. K. Klosterman and M. Fujita, *Angew. Chem., Int. Ed.*, 2009, **48**, 3418.
6 E. C. Constable in *Supramolecular Chemistry: From Molecules to Nanomaterials*, ed. P. A. Gale and J. W. Steed, Wiley, 2012, vol. 6, p. 3073.
7 M. O'Keefe and O. M. Yaghi, *Chem. Rev.*, 2012, **112**, 675.
8 E. C. Constable, *Pure Appl. Chem.*, 1996, **68**, 253.
9 E. C. Constable, *Chem. Soc. Rev.*, 2007, **36**, 246.
10 C. E. Housecroft, *Dalton Trans.*, 2014, **43**, 6594.
11 X. Tan, X. Chen, J. Zhang and C.-Y. Song, *Dalton Trans.*, 2012, **41**, 3616; L. Wen, X. Ke, L. Qiu, Y. Zou, L. Zhou, J. Zhao and D. Li, *Cryst. Growth Des.*, 2012, **12**, 4083; W. Yang, A. J. Davies, X. Lin, M. Suyetin, R. Matsuda, A. J. Blake, C. Wilson, W. Lewis, J. E. Parker, C. C. Tang, M. W. George, P. Hubberstey, S. Kitagawa, H. Sakamoto, E. Bichoutskaia, N. R. Champness, S. Yang and M. Schröder, *Chem. Sci.*, 2012, **3**, 2992; Y.-Q. Chen, S.-J. Liu, Y.-W. Li, G.-R. Li, K.-H. He, Y.-K. Qu, T.-L. Hu and X.-H. Bu, *Cryst. Growth Des.*, 2012, **12**, 5426; P. Yang, M.-S. Wang, J.-J. Shen, M.-X. Li, Z.-X. Wang, M. Shao and X. He, *Dalton Trans.*, 2014, **43**, 1460; Y.-L. Gai, F.-L. Jiang, L. Chen, Y. Bu, M.-Y. Wu, K. Zhou, J. Pan and M.-C. Hong, *Dalton Trans.*, 2013, **42**, 9954; Y.-Q. Chen, G.-R. Li, Y.-K. Qu, Y.-H. Zhang, K.-H. He, Q. Gao and X.-H. Bu, *Cryst. Growth Des.*, 2013, **13**, 901; Y. Li, Z. Ju, B. Wu and D. Yuan, *Cryst. Growth Des.*, 2013, **13**, 4125; F. Yuan, J. Xie, H.-M. Hu, C.-M. Yuan, B. Xu, M.-L. Yang, F.-X. Dong and G.-L. Xue, *CrystEngComm*, 2013, **15**, 1460; F. Yuan, Q. Zhu, H.-M. Hu, J. Xie, B. Xu, C.-M. Yuan, M.-L. Yang, F.-X. Dong and G.-L. Xue, *Inorg. Chim. Acta*, 2013, **397**, 117; H.-N. Zhang, F. Yuan, H.-M. Hu, S.-S. Shen and G.-L. Xue, *Inorg. Chem. Commun.*, 2013, **34**, 51; E. C. Constable, G. Zhang, C. E. Housecroft and J. A. Zampese, *CrystEngComm*, 2011, **13**, 6864; J. Heine, J. Schmedt auf der Günne and S. Dehnen, *J. Am. Chem. Soc.*, 2011, **133**, 10018; V. N. Dorofeeva, S. V. Kolotilov, M. A. Kiskin, R. A. Polunin, Z. V. Dobrokhotova, O. Cador, S. Golhen, L. Ouahab, I. L. Eremenko and V. M. Novotortsev, *Chem. – Eur. J.*, 2012, **18**, 5006; K.-R. Ma, F. Ma, Y.-L. Zhu, L.-J. Yu, X.-M. Zhao, Y. Yang and W.-H. Duan, *Dalton Trans.*, 2011, **40**, 9774.
12 E. C. Constable, C. E. Housecroft, P. Kopecky, M. Neuburger, J. A. Zampese and G. Zhang, *CrystEngComm*, 2012, **14**, 446.
13 E. C. Constable, G. Zhang, C. E. Housecroft and J. A. Zampese, *Inorg. Chem. Commun.*, 2012, **15**, 113.
14 Y. M. Klein, E. C. Constable, C. E. Housecroft, J. A. Zampese and A. Crochet, *CrystEngComm*, 2014, **16**, 9915.

15 E. C. Constable, C. E. Housecroft, S. Vujovic and J. A. Zampese, *CrystEngComm*, 2014, **16**, 3494.
16 Y. M. Klein, E. C. Constable, C. E. Housecroft and A. Prescimone, *CrystEngComm*, 2015, **17**, 2070.
17 E. C. Constable, C. E. Housecroft, M. Neuburger, J. Schönle, S. Vujovic and J. A. Zampese, *Polyhedron*, 2013, **60**, 120.
18 E. C. Constable, G. Zhang, E. Coronado, C. E. Housecroft and M. Neuburger, *CrystEngComm*, 2010, **12**, 2139.
19 E. C. Constable, C. E. Housecroft, S. Vujovic, J. A. Zampese, A. Crochet and S. R. Batten, *CrystEngComm*, 2013, **15**, 10068.
20 V. Auger and I. Robin, *Comptes Rendus*, 1924, **178**, 1546.
21 O. M. Yaghi, M. O'Keeffe, N. W. Ockwig, H. K. Chae, M. Eddaoudi and J. Kim, *Nature*, 2003, **423**, 705.
22 E. C. Constable, G. Zhang, C. E. Housecroft, M. Neuburger and J. A. Zampese, *CrystEngComm*, 2009, **11**, 2279.
23 Y. M. Klein, E. C. Constable, C. E. Housecroft and A. Prescimone, *Inorg. Chem. Commun.*, 2014, **49**, 41.
24 E. C. Constable, G. Zhang, C. E. Housecroft, M. Neuburger and J. A. Zampese, *CrystEngComm*, 2010, **12**, 3733.
25 *APEX2, version 2 User Manual, M86-E01078*, Bruker Analytical X-ray Systems, Inc., Madison, WI, 2006.
26 P. W. Betteridge, J. R. Carruthers, R. I. Cooper, K. Prout and D. J. Watkin, *J. Appl. Crystallogr.*, 2003, **36**, 1487.
27 I. J. Bruno, J. C. Cole, P. R. Edgington, M. K. Kessler, C. F. Macrae, P. McCabe, J. Pearson and R. Taylor, *Acta Crystallogr., Sect. B: Struct. Sci.*, 2002, **58**, 389.
28 C. F. Macrae, I. J. Bruno, J. A. Chisholm, P. R. Edgington, P. McCabe, E. Pidcock, L. Rodriguez-Monge, R. Taylor, J. van de Streek and P. A. Wood, *J. Appl. Crystallogr.*, 2008, **41**, 466.
29 V. A. Blatov and A. P. Shevchenko, *TOPOS Professional v. 4.0*, Samara State University, Russia.
30 A. L. Spek, *Acta Crystallogr., Sect. D: Biol. Crystallogr.*, 2009, **65**, 148.
31 N. Yoshikawa, S. Yamabe, N. Kanehisa, H. Takashima and K. Tsukahara, *J. Phys. Org. Chem.*, 2009, **22**, 410.
32 N. Yoshikawa, S. Yamabe, N. Kanehisa, T. Inoue, H. Takashima and K. Tsukahara, *J. Phys. Org. Chem.*, 2010, **23**, 431.
33 T. Mutai, H. Satou and K. Araki, *Nat. Mater.*, 2005, **4**, 685.
34 E. C. Constable, G. Zhang, C. E. Housecroft, M. Neuburger and J. A. Zampese, *CrystEngComm*, 2010, **12**, 2146.
35 L. Hou and D. Li, *Inorg. Chem. Commun.*, 2005, **8**, 190.
36 See for example: W. Li, H.-P. Jia, Z.-F. Ju and J. Zhang, *Cryst. Growth Des.*, 2006, **6**, 2136; G.-X. Jin, J.-P. Ma and Y.-B. Dong, *J. Mol. Struct.*, 2013, **1052**, 146; C.-M. Che, C.-W. Wan, K.-Y. Ho and Z.-Y. Zhou, *New J. Chem.*, 2001, **25**, 63.

